

PSDiff: Diffusion Model for Person Search with Iterative and Collaborative Refinement

Chengyou Jia, Minnan Luo*, Zhuohang Dang Guang, Dai, Xiaojun Chang, Jingdong Wang, and Qinghua Zheng

Abstract—Dominant Person Search methods aim to localize and recognize query persons in a unified network, which jointly optimizes two sub-tasks, *i.e.*, detection and Re-Identification (ReID). Despite significant progress, two major challenges remain: 1) Detection-prior modules in previous methods are sub-optimal for the ReID task. 2) The collaboration between two sub-tasks is ignored. To alleviate these issues, we present a novel Person Search framework based on the Diffusion model, PSDiff. PSDiff formulates the person search as a dual denoising process from noisy boxes and ReID embeddings to ground truths. Unlike existing methods that follow the Detection-to-ReID paradigm, our denoising paradigm eliminates detection-prior modules to avoid the local-optimum of the ReID task. Following the new paradigm, we further design a new Collaborative Denoising Layer (CDL) to optimize detection and ReID sub-tasks in an iterative and collaborative way, which makes two sub-tasks mutually beneficial. Extensive experiments on the standard benchmarks show that PSDiff achieves state-of-the-art performance with fewer parameters and elastic computing overhead.

Index Terms—Person Search, Diffusion Model, Person Re-identification, Object Detection

I. INTRODUCTION

PERSON Search [1], [2] aims to locate and recognize query persons in a gallery of unconstrained scene images, which consists of two sub-tasks, *i.e.*, detection and Re-Identification (ReID). Because of acting on the whole scene images, person search shows more potential than the ReID task [3]–[6] in real-world applications, such as criminal tracking, person behavior analysis and human-computer interaction. Early approaches [2], [7] adopt the two-stage paradigm that tackles two sub-tasks separately. In detail, a detector is applied to scene images to predict the bounding boxes and then a followed ReID network extracts ReID embeddings from the detected person slices. In contrast, end-to-end methods [1], [8]–[14] aim to localize and recognize query persons in

*Corresponding author: Minnan Luo.

Chengyou Jia, Minnan Luo, Zhuohang Dang and Qinghua Zheng are with the School of Computer Science and Technology, Xi’an Jiaotong University, and Key Laboratory of Intelligent Networks and Network Security (Xi’an Jiaotong University), Ministry of Education, Xi’an, Shaanxi 710049, China, e-mail: {cp3jia,dangzhuohang}@stu.xjtu.edu.cn, {qhzheng,minnluo}@mail.xjtu.edu.cn.

Guang Dai is with SGIT AI Lab, and also with State Grid Shaanxi Electric Power Company Limited, State Grid Corporation of China, Shaanxi, China, e-mail: guang.gdai@gmail.com.

Xiaojun Chang is with the Faculty of Information Technology, University Of Technology Sydney, Australia. Xiaojun Chang is also a Visiting Professor with Department of Computer Vision, Mohamed bin Zayed University of Artificial Intelligence (MBZUAI). e-mail: cxj273@gmail.com.

Jingdong Wang is with the Baidu Inc, China, e-mail: wangjingdong@outlook.com.



Fig. 1: (a) The baseline with detection-prior modules ignores some crucial parts such as carry-on items, causing low ReID matching scores. (b) The baseline without collaboration misses results with high ReID matching scores due to inaccurate positions and low confidence scores. In comparison, our method can increase discriminative parts and refine two tasks collaboratively, producing more discriminative embeddings and more accurate detection results. “D” and “R” index confidence scores of detection and ReID matching scores with queries, respectively. The bounding boxes in green and red denote the correct and wrong results.

a unified network, which is more concise and efficient in general. Due to their advantages, end-to-end methods became the dominant fashion and attracted the attention of researchers.

Although previous end-to-end methods have made significant progress, two major challenges still remain. (1) **Detection-prior modules in previous methods are suboptimal for the ReID task.** Existing end-to-end methods [1], [9], [10], [12]–[14] are first built on traditional detectors, like Faster-RCNN [15] or DETR [16], which inevitably bring detection-prior modules to the person search framework. Specifically, Faster-RCNN introduces the Region Proposal Network (RPN) to generate high-quality region proposals and DETR proposes learnable object queries to learn potential positions. The purpose of these detection-prior modules is to learn proposals of persons in advance according to given annotations. As shown in Fig. 1 (a), some crucial parts, which possess the discriminative information, are essential for ReID matching but may be ignored, leading to unsatisfactory ReID matching scores. (2) **The collaboration between two sub-tasks is ig-**

nored. Existing methods [1], [9], [10] only follow the principle that more accurate detection results contribute more to the learning of ReID tasks but ignore that better ReID clues can also bring more high-quality detection results. Fig. 1 (b) shows detection candidates with low confidences and inaccurate positions can be effectively improved by high ReID matching scores. Therefore, two sub-tasks should collaboratively work to benefit each other.

Inspired by [17]–[19], we address the aforementioned issues by designing a novel **Person Search** framework based on the **Diffusion** model, called **PSDiff**. Innovatively, we formulate the person search task as a dual denoising process from noisy boxes and ReID embeddings to ground truths. Specifically, during the training stage, both object boxes and ReID embeddings diffuse from ground truths to randomly distributed noises by a designed dual noise generator. Then, the model learns a novel Collaborative Denoising Layer (CDL) to reverse the noising process. The proposed CDL generates collaborative features by interacting features from two sub-tasks and then predicts results with a cascaded architecture. During the inference stage, the trained CDL iteratively and collaboratively refines a set of randomly generated boxes and ReID embeddings. In summary, unlike previous methods that follow the Detection-to-ReID paradigm, our denoising paradigm eliminates detection-prior modules and can refine predictions with iterative collaboration.

We evaluate the PSDiff on CUHK-SYSU and PRW datasets. With ResNet-50 and Swin-Base, PSDiff achieves 95.1% and 95.7% mAP on CUHK-SYSU, and 53.5% and 57.1% mAP on PRW, outperforming existing methods. Besides, our approach also shows several appealing properties, *i.e.*, fewer parameters and elastic computing overhead.

Our main contributions are summarized as follows:

- We propose **PSDiff**, a novel person search framework based on the diffusion model. By formulating the person search task as a dual denoising process, PSDiff successfully addresses challenges in previous works, *i.e.*, destructive detection-prior modules and missing collaboration. To our knowledge, PSDiff is the first study to apply the diffusion model to person search.
- We propose the Collaborative Denoising Layer (CDL), which aims to denoise noisy boxes and ReID embeddings. Following the denoising paradigm, the trained CDL can be reused to refine predictions in an iterative and collaborative way.
- The extensive experiments on the standard benchmarks, including CUHK-SYSU and PRW, show that PSDiff achieves state-of-the-art performance. What’s more, PSDiff also shows several appealing properties about parameters and computing overhead.

The remainder of the article is organized as follows. In Section II, we briefly summarize the related works, *e.g.*, person search and diffusion model. Section III introduces the formulation of diffusion models. In Section IV, we describe the proposed PSDiff in detail. In Sections V, we first present datasets and implementation details and then report experimental results comparing with SOTA methods. We also conduct the ablation study and provide more detailed analysis.

Section VI concludes this paper and describes some ethical considerations of this work.

II. RELATED WORK

A. Person Search

Recently, person search has attracted much attention from the computer vision community because of its potential in real-world applications, such as criminal tracking [20], person behavior analysis [21] and human-computer interaction [22]–[24]. Existing solutions to person search generally fall into two categories: two-stage methods and end-to-end methods.

1) *Two-stage methods*: these methods [2], [7], [25], [26] tackle detection and ReID tasks separately. They employ the independent detector and ReID network to predict the bounding boxes and extract ReID features, respectively. Zheng *et al.* [2] pioneered a two-stage framework and evaluated the method on various combinations of different detectors [27]–[29] and ReID networks [3]–[6]. They further proposed the Confidence Weighted Similarity (CWS) to integrate detection confidence into the process of similarity matching. Han *et al.* [25] proposed a ReID-driven localization refinement framework, which employs the supervision of ReID loss to produce more reliable bounding boxes. Wang *et al.* [26] further pointed out the consistency problem that the ReID model trained with ground-truth bounding boxes is unreliable and proposed a task-consistent framework by producing query-like bounding boxes to alleviate this issue. In general, two-stage methods focus on how to learn more discriminative Re-ID features based on the detection results. Despite the excellent performance, two-stage methods always suffer from terrible efficiency due to the requirement of training and inference with two networks.

2) *End-to-end methods*: Xiao *et al.* [1] first proposed an end-to-end framework by employing the Faster RCNN as the detector and sharing base layers with the ReID network. After that, end-to-end methods have attracted the attention of researchers and have been the dominant fashion [8]–[14]. NAE [9] proposed to disentangle the person embedding into norm and angle for balancing two conflicting sub-tasks. Li *et al.* [10] proposed a Sequential End-to-end Network (SeqNet), which tackles this problem with two sequential sub-networks (detector and ReID module) and refines the predicted bounding boxes of the early stage. Furthermore, Yan *et al.* [11] first employed the anchor-free framework to avoid the high computational overhead from dense object anchors. They further introduced an aligned feature aggregation module to address the misalignment issues in scale, region, and task levels. Recently, transformer-based detectors like DETR have made significant progress. Cao *et al.* [13] introduced a novel transformer-based person search framework. They treated the person search as a set prediction problem and introduced a part attention block to capture the relationship of different parts.

In this paper, we propose a novel diffusion-based person search framework. Innovatively, we formulate the person search task as a dual denoising process, effectively addressing the limitations of previous approaches by eliminating the detection-prior module.

B. Diffusion Model

The class of diffusion-based (or score-based) models has recently become one of the hottest topics in computer vision. Deep diffusion-based generative models [17], [30] have demonstrated their remarkable performance in terms of the quality and diversity of the generated samples. So far, diffusion models have been applied to a wide variety of generative tasks, including Image Generation [31], [32], Image Editing [33], Image Super-Resolution [34] *etc.* In addition to the generative fields, recent methods also explore the potential of diffusion models for discriminative tasks. Some pioneer works tried to adopt the diffusion model for image segmentation [18], [35], [36]. Moreover, Han *et al.* [37] approached supervised learning from a conditional generation perspective and first applied the diffusion model to classification and regression. Chen *et al.* [19] further adopted the diffusion model for object detection by formulating this task as a generative denoising process. What's more, diffusion models have also shown promising results in detecting anomalies in medical images [38]–[40]. These excellent works confirm the wide-ranging applicability of diffusion models, indicating that there may be even more untapped applications waiting to be explored.

In general, diffusion models for discriminative tasks follow Noise-to-Label paradigm that supervises learning labels from a conditional generation perspective and denoises the random noise to the ground-truth. This paper extends this paradigm to a novel pipeline (DualNoises-to-DualLabels) by applying the diffusion model to the person search task.

III. PRELIMINARIES OF THE DIFFUSION MODEL

In this section, we introduce the formulation of the diffusion model in detail. Diffusion models are a class of probabilistic generative models, which first gradually add noise to an image until it becomes completely degraded into noise and then learn to reverse the noisy data structure. Thus, the training procedure is divided into two processes: a **forward noising process** and a **reverse denoising process**.

The forward process that gradually adds Gaussian noise to data $x_0 \sim q(x_0)$ over the course of T timesteps

$$q(x_{1:T}|x_0) = \prod_{t=1}^T q(x_t|x_{t-1}), \quad (1)$$

$$q(x_t|x_{t-1}) = \mathcal{N}(x_t; \sqrt{1 - \beta_t}x_{t-1}, \beta_t I), \quad (2)$$

where hyper-parameters β_t are set so that x_T is approximately distributed according to a standard normal distribution, *i.e.*, $p(x_T) = \mathcal{N}(0, I)$. By leveraging the above properties, the reverse process aims to generate new samples from $p_\theta(x_0) = \int p_\theta(x_{0:T}) dx_{1:T}$, where

$$p_\theta(x_{0:T}) = p(x_T) \prod_{t=1}^T p_\theta(x_{t-1} | x_t), \quad (3)$$

$$p_\theta(x_{t-1} | x_t) = \mathcal{N}(x_{t-1}; \mu_\theta(x_t, t), \Sigma_\theta(x_t, t)), \quad (4)$$

where μ_θ and Σ_θ are the mean and the diagonal covariance matrix to be predicted. Then, this reverse process is trained

to match the joint distribution of the forward process by optimizing the evidence lower bound:

$$L_\theta(x_0) = \mathbb{E}_q \left[\sum_{t>1} D_{\text{KL}}(q(x_{t-1} | x_t, x_0) \| p_\theta(x_{t-1} | x_t)) + L_T(x_0) - \log p_\theta(x_0 | x_1) \right], \quad (5)$$

where $L_T(x_0) = D_{\text{KL}}(q(x_T, x_0) \| p(x_T))$. The forward process posteriors $q(x_{t-1}|x_t, x_0)$ and marginals $q(x_t|x_0)$ are Gaussian, and the KL divergences in the ELBO can be calculated in closed form. Thus it is possible to train the diffusion model by taking stochastic gradient steps on random terms of Eq. (5).

Conditional Diffusion Model: recent researches [34], [41], [42] proposed the conditional diffusion model as an extension of the above unconditional diffusion models [17], [30], [43], which aims to bring the prior knowledge to the reverse denoising process. The conditional diffusion model involves a conditional signal c that is associated with the data x_0 , such as a label in the context of class-conditional generation, or a low-resolution image in the context of super-resolution [34], [41], [42]. In conditional diffusion models, the goal of the reverse process is to learn a conditional model:

$$p_\theta(x_{t-1}|x_t, c) = \mathcal{N}(x_{t-1}; \mu_\theta(x_t, c, t), \Sigma_\theta(x_t, c, t)). \quad (6)$$

IV. METHODOLOGY

In this section, we begin by reformulating the person search task under the diffusion process. Next, we provide details of our model architecture to explain how to achieve the new formulation. After that, we elaborate the process of training and inference. Finally, we provide some discussions on the comparison between our method and previous methods.

A. Diffusion Process for Person Search

The person search task tends to train the model to learn pairs (S, \hat{b}, \hat{e}) , where S indexes scene images and \hat{b}, \hat{e} are predicted locations and discriminative embeddings of all possible persons, respectively. In this paper, we reformulate the task as the diffusion processes, including a dual forward noising process and a dual reverse denoising process.

1) **Forward noising process:** Given ground truths of bounding boxes b_0 and ReID embedding e_0 , our dual forward noising process q gradually adds Gaussian noise to construct noisy labels. Especially, the forward process is independent of the given condition c as [34], [41], [42]. The process is specified as follows:

$$\begin{aligned} q(b_t|b_0, c) &= q(b_t|b_0) = \mathcal{N}(b_t; \sqrt{\bar{\alpha}_t}b_0, (1 - \bar{\alpha}_t)I), \\ q(e_t|e_0, c) &= q(e_t|e_0) = \mathcal{N}(e_t; \sqrt{\bar{\alpha}_t}e_0, (1 - \bar{\alpha}_t)I), \end{aligned} \quad (7)$$

where $t \sim \text{Uniform}(\{1, \dots, T\})$ is the time step sampled from the number of diffusion steps T . $\bar{\alpha}_t = \prod_{i=1}^t \alpha_i$ is controlled by the noise variance schedule [44]. b_t and e_t refer to the noisy boxes and embeddings respectively.

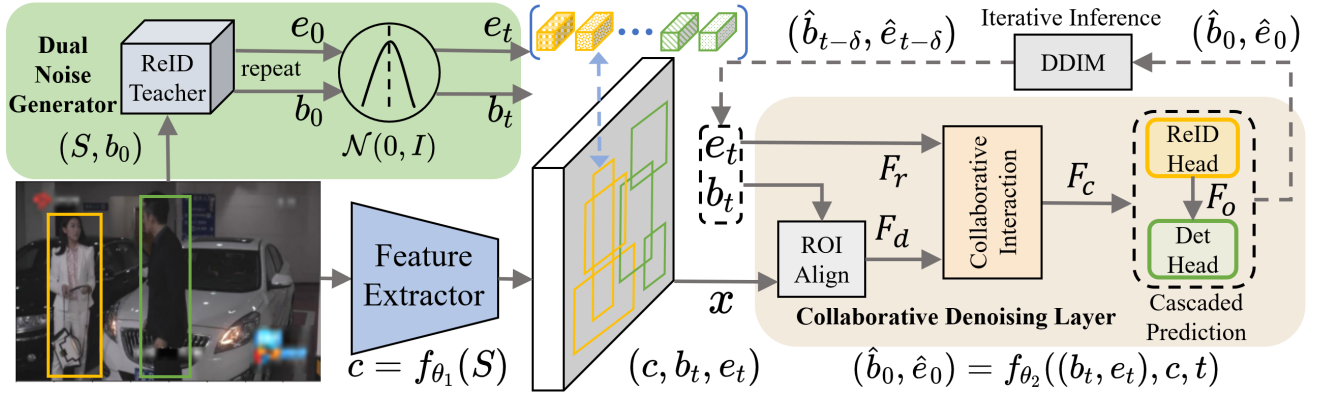


Fig. 2: The overall architecture of the proposed PSDiff. During the training stage, b_t, e_t are noisy boxes and embeddings calculated by Eq. (10). During the inference stage, b_t, e_t are randomly generated boxes and ReID embeddings from Gaussian noises, which are refined gradually by the iterative inference with fast sampling methods, e.g., DDIM.

2) *Reverse denoising process*: Given noisy boxes b_t and noisy ReID embeddings e_t , the goal of the reverse denoising process is to learn a conditional model:

$$p_\phi(\{b_{t-1}, e_{t-1}\} | \{b_t, e_t\}, c) = \mathcal{N}(\{b_{t-1}, e_{t-1}\}; \mu_\phi(\{b_t, e_t\}, c, t), \Sigma_\phi(\{b_t, e_t\}, c, t)), \quad (8)$$

where μ_ϕ and Σ_ϕ are the mean and diagonal covariance matrix to be predicted [17], [45]. Specifically, Σ_ϕ is predefined without learning and a neural network $f_{\theta_2}((b_t, e_t), c, t)$ is employed to indirectly approximate μ_ϕ by predicting \hat{b}_0, \hat{e}_0 collaboratively. This step-by-step denoising framework enables PSDiff to refine \hat{b}_0, \hat{e}_0 in an iterative and collaborative way. In the following, we provide details of our model architecture to explain how to achieve the above procedure.

B. Model Architecture

The overview of the proposed framework is presented in Fig. 2. The model consists of three main components: (1) *feature extractor*, (2) *dual noise generator* and (3) *collaborative denoising layer*. The feature extractor first generates conditional features c from the input image. Then the dual noise generator samples the timestep t and transforms ground truths to noisy boxes b_t and noisy embeddings e_t . Finally, the collaborative denoising layer receives dual noises and their condition c, t to predict \hat{b}_0, \hat{e}_0 . We will elaborate on each component in the following subsections.

1) *Feature Extractor*: The feature extractor aims to extract high-level and multi-scale conditional features c from raw scene images S . This process is specified as follows:

$$c = f_{\theta_1}(S). \quad (9)$$

Specifically, we implement f_{θ_1} with Feature Pyramid Network (FPN) [46] based on both CNN-based ResNet [47] and Transformer-based Swin [48] architecture as [19].

2) *Dual Noise Generator*: The dual noise generator is designed to corrupt boxes and embeddings from ground truths to randomly distributed noises. We first repeat the ground truth boxes and corresponding embeddings to a fixed number N_{train} for each image. Then, we sample timesteps $t \sim$

$\text{Uniform}(\{1, \dots, T\})$ and the noisy boxes and embeddings are generated by adding Gaussian noises as follows:

$$\begin{aligned} q(b_t | b_0, c) &= s_1 \sqrt{\alpha_t} (b_0 * 2 - 1) + \sqrt{(1 - \alpha_t)} \epsilon_1, \\ q(e_t | e_0, c) &= s_2 \sqrt{\alpha_t} \text{Norm}(e_0) + \sqrt{(1 - \alpha_t)} \epsilon_2, \end{aligned} \quad (10)$$

where $\epsilon_1, \epsilon_2 \sim \mathcal{N}(0, I)$. Operations $b_0 * 2 - 1$ and $\text{Norm}(e_0)$ aim to rescale the ground truths into $[-1, 1]$. s_1 and s_2 are the signal-to-noise ratios (SNR) corresponding to b_0 and e_0 , respectively. The SNR further adjusts the scaling factor, which has a significant effect on the performance [19], [36]. Besides, we keep the noise scalar α_t consistent for both b_0 and e_0 .

How to get the ground truth of embeddings e_0 ? Note that there are only person identities in the original annotations. In this work, we first use annotations of bounding box and identity to train a ReID teacher model as [49], [50]. Then, we adopt a strategy of feature imitation to take the output of the ReID teacher model as the ground truth of embeddings e_0 . This process is specified as follows:

$$e_0 = \text{Teacher}(S, b_0). \quad (11)$$

Note that the ReID teacher model is pre-trained and only used in the training phase of PSDiff. It will be removed during inference and thus will not bring an extra computational burden. Specifically, we employ the supervised HHCL [49], [50] as the teacher model in PSDiff, which offers two distinct advantages. First, it employs hard-sample mining to focus on challenging examples, thereby enhancing the learning process. Second, it leverages unlabeled samples as CCR [49] to enrich the training set. These benefits collectively contribute to improving the quality of the learned embeddings, bringing them closer to the ground truth distribution of embeddings. We next discuss how one can learn a neural network to reverse this Gaussian diffusion process.

3) *Collaborative Denoising Layer*: Given noisy boxes b_t and embeddings e_t , we propose the Collaborative Denoising Layer (CDL) to predict \hat{b}_0, \hat{e}_0 as:

$$(\hat{b}_0, \hat{e}_0) = f_{\theta_2}((b_t, e_t), c, t), \quad (12)$$

where \hat{b}_0, \hat{e}_0 refer to the predicted boxes and embeddings, respectively. As shown in Fig. 2, CDL first utilizes the ROIAlign

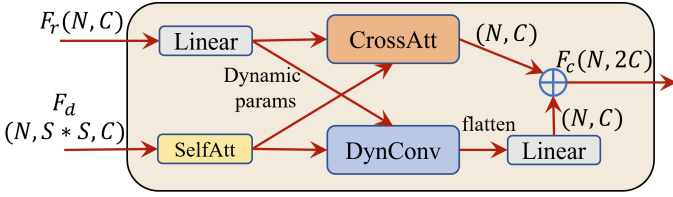


Fig. 3: Illustrations of the collaborative interaction.

operation to extract detection features, *i.e.*, $F_d(N, S * S, C)$ for N noisy boxes¹, where S, C is the size and the channel of features. Then CDL generates the collaborative features, *i.e.*, F_c , by collaboratively interacting F_d and ReID embeddings, *i.e.*, $F_r(N, C)$ to realize the complementary advantages of the two sub-tasks. After the collaborative interaction, F_c is used to predict results.

(a) Collaborative interaction: we present the details of the collaborative interaction in Fig. 3. We first apply a linear layer and a multi-head self-attention module to F_r and F_d , separately. The former generates dynamic kernel parameters and the latter aims to model intra-level visual relationships [51], [52]. Then the new F_d is enhanced by a dynamic convolution, whose kernel parameters are produced by F_r . Meanwhile, we apply the cross-attention module to F_r and F_d , where F_r serves as queries and F_d serve as keys and values. The above collaborative interaction reinforces features of one task by embedding information from the other task. Finally, two kinds of improved features are concatenated as $F_c(N, 2C)$ to predict results.

(b) Cascaded prediction: previous detectors always adopt the iterative structure [52], [53] to improve the performance, where the newly generated object boxes and object features will serve as the next stage’s proposal boxes and proposal features. Object features, *i.e.*, F_o , refer to the high dimensional intermediate features used to predict boxes. Sparse R-CNN [52] further confirmed that iteratively optimizing F_o matters while only updating the boxes does not make a big difference. However, in our framework, only predicted boxes and ReID embeddings are passed to the next iterative process. Therefore, we design a cascaded architecture instead of a common parallel structure [1], [10] to further refine F_o . As shown in Fig. 2, the F_c are first used to predict embeddings \hat{e}_0 . Then we take $F_o = \hat{e}_0$ and feed F_o to the detection head for predicting \hat{b}_0 . This design makes sense, due to the fact that the dimension of e_0 is much larger than b_0 in general, *i.e.*, 4 for $b_0 \ll 256$ for e_0 . With the iterative refinement of ReID embeddings, this strategy ensures that both F_r and F_o are rectified, leading to more accurate detection results.

C. Training and Inference

1) **Training process:** We adopt an end-to-end training mechanism. The model takes N_{train} noisy boxes and embeddings as input and then predicts N_{train} box coordinates and ReID embeddings for each image. The pseudo-code of the

¹Note that we generate N_{train} noisy boxes for each image, and the number of boxes in one batch is $N = N_{train} * batchsize$.

Algorithm 1 Training process of PSDiff

Input total diffusion steps T , dataset D , pretrained ReID teacher network

repeat

1. Sample data $(S, b_0) \sim D$;
2. Sample $t \sim \text{Uniform}(\{1, \dots, T\})$, $\epsilon_1, \epsilon_2 \sim \mathcal{N}(0, I)$;
3. Compute condition x using f_{θ_1} by Eq. (9);
4. Compute e_0 using teacher network by Eq. (11);
5. Repeat b_0, e_0 and compute b_t, e_t by Eq. (10);
6. Predict \hat{b}_0, \hat{e}_0 using f_{θ_2} by Eq. (12);
7. Take gradient step on loss \mathcal{L} by Eq. (13);

until convergence

Algorithm 2 Inference process of PSDiff

Input total diffusion steps T , inference space δ , image S , $\hat{b}_T, \hat{e}_T \sim \mathcal{N}(0, I)$

- 1: **for** $t = T, T - \delta, \dots, T - k\delta, \dots$ **do**
- 2: 1. Compute condition x using f_{θ_1} by Eq. (9);
- 3: 2. Compute \hat{b}_0, \hat{e}_0 using $f_{\theta_2}((\hat{b}_t, \hat{e}_t), x, t)$ by Eq. (12);
- 4: **if** $t > \delta$ **then**
- 5: 3. Compute $\hat{b}_{t-\delta}, \hat{e}_{t-\delta}$ from newly predicted \hat{b}_0, \hat{e}_0 using the fast sampling method;
- 6: **else**
- 7: **return** \hat{b}_0, \hat{e}_0
- 8: **end if**
- 9: **end for**

detailed training process is shown in Algorithm 1. In this work, we extend the set prediction loss [16], [54] to the person search task for training our diffusion-based model. The extended loss produces an optimal bipartite matching between predictions and ground truths as previous methods [16], [54]. Differently, the matching cost is defined as

$$\mathcal{L} = \underbrace{\lambda_{cls}\mathcal{L}_{cls} + \lambda_{L1}\mathcal{L}_{L1} + \lambda_{giou}\mathcal{L}_{giou}}_{denoise:b_t} + \underbrace{\lambda_{reid}\mathcal{L}_{reid}}_{denoise:e_t}, \quad (13)$$

where λ_{cls} , λ_{giou} , λ_{L1} and λ_{reid} are coefficients of each component. \mathcal{L}_{cls} , \mathcal{L}_{L1} and \mathcal{L}_{giou} denote the focal loss [55], ℓ_1 loss and generalized IoU loss [56] respectively. We calculate these losses as the previous methods [16], [52] of object detection. In addition, losses for denoising e_t are defined as

$$\mathcal{L}_{reid} = \sum_{i=1}^M \|e_0^i - \hat{e}_0^{\sigma(i)}\|_2, \quad (14)$$

where i is the index of ground truths and $\sigma(i)$ is the index of bipartite matching results corresponding to i . M is the number of ground truths for each image. We employ the ℓ_2 loss to supervise predicted ReID embeddings \hat{e}_0 with e_0 .

2) **Inference via Iterative Refinement:** The inference procedure of PSDiff is a denoising process, starting from N_{test} Gaussian noises $\hat{b}_T, \hat{e}_T \sim \mathcal{N}(0, I)$. The model refines predictions in an iterative way under the sampling strategy, *i.e.*, $(\hat{b}_T, \hat{e}_T) \rightarrow (\hat{b}_{T-\delta}, \hat{e}_{T-\delta}) \rightarrow \dots \rightarrow (\hat{b}_0, \hat{e}_0)$, where δ is the inference space. In each step, the refined boxes and embeddings from the last step are sent into the CDL to denoise gradually. However, traditional step-by-step inference usually

needs thousands of sequential steps of CDL evaluations, thereby giving rise to a much slower inference speed than previous person search methods. Therefore, we employ some fast sampling methods, *e.g.*, DDIM [45], DPM-solver [57] and DPM-solver++ [58] to accelerate the inference. The pseudo-code of the inference process is shown in Algorithm ??.

D. Discussion

In this section, we provide some discussions, primarily focusing on the distinctions and comparisons between our method and previous approaches. Specifically, we compare our diffusion-based framework with methods that are built upon Faster-RCNN or DETR architectures. Additionally, we discuss how our approach stands in relation to methods that employ knowledge distillation techniques.

1) *Comparison to methods with other detectors:* previous person search approaches have traditionally relied on established detectors that involve predefined object candidates, *e.g.*, empirical object priors in Faster-RCNN [15] and learnable object queries in DETR [16]. These hand-designed or pre-learned object candidates inadvertently prioritize object detection over ReID, leading to sub-optimal performance in the ReID task and hindering effective collaboration between the two tasks. In contrast, our diffusion-based method eliminates such detection-prior modules. Instead, it commences from random object boxes and ReID embeddings, enabling a collaborative optimization for the entire person search task. It's worth noting that while our method bears some resemblance to RDLC [25], their primary focus is on mitigating detector bias in two-stage methods. Our approach, conversely, targets the elimination of detection-prior in end-to-end methods, which can be considered as a further advancement upon their work.

2) *Comparison to methods with knowledge distillation:* previous approaches [59], [60] pointed out that the performance bottleneck in end-to-end person search models arises from the feature map containing redundant contextual information. To mitigate this issue, they employ Knowledge Distillation (KD) to provide superior prior knowledge. In our work, we adopt a similar strategy by leveraging the output of the pre-trained ReID teacher to approximate the ground truth of embeddings. Our model is specifically trained to recover accurate embeddings from their noise-corrupted versions. Although the form of our loss function shares similarities with KD-based methods, our approach offers a unique advantage: it enables iterative refinement of the predicted embeddings during the inference stage. This sets our method apart from existing approaches, which primarily focus on rigid mimicking the output of the ReID teacher. Experimental results substantiate that our method surpasses previous KD-based strategies, especially in terms of transferability.

V. EXPERIMENTS

In this section, we empirically evaluate the performance of PSDiff on two benchmark datasets. We also provide detailed ablation studies to illustrate how each component of our method works. Furthermore, we conduct case studies to better illustrate the effectiveness of our method.

A. Experimental Setup

1) *Dataset:* We empirically evaluate the effectiveness of the proposed framework over two standard benchmarks.

- **CUHK-SYSU [1]** is a large-scale dataset that is collected from street snaps or movies, including 18,184 images and 96,143 annotated pedestrian bounding boxes (23,430 boxes are ID labeled from 8,432 identities). These images cover significant variations of viewpoints, lighting and background conditions. The training set consists of 11,206 images from 5,532 identities, while the testing set contains 2,900 query images and 6,978 gallery images. We report the results with the default gallery size of 100 if not specified.
- **PRW [2]** is extracted from six surveillance cameras on a university campus, including 11,816 video frames and 43,110 bounding boxes (34,304 boxes are ID labeled from 932 identities). PRW is more challenging because each identity has more instances (36.8 *vs.* 2.8 in CUHK-SYSU), making retrieving difficult. The training set consists of 5,704 frames and 482 identities, while the testing set includes 6,112 gallery images and 2,057 query images from 450 different identities.

2) *Evaluation Protocol:* We report the performance of the person search in terms of the Cumulative Matching Characteristic (CMC) and the mean Average Precision (mAP). CMC is the most popular evaluation metric for re-identification, where matching is considered correct only if the IoU between the ground truth bounding box and the matching box is larger than 0.5. The mAP reflects the accuracy of localizing the query in the gallery, where the AP score of searching a query from gallery images is calculated first and then AP scores are averaged across all the queries to calculate the mAP. We also report the detection performance under the mAP50 metric.

3) *Implementation Details:* The feature extractor in our network adopts the ResNet-50 [47] and Swin-Base [48] pre-trained on the ImageNet dataset, together with the FPN [46]. The dual noise generator adopts the monotonically decreasing cosine schedule for α_t in different timesteps as in [44]. The denoising layer (CDL) is initialized with Xavier init [61]. For the ReID teacher model, We strictly adhere to the settings outlined in HHCL [50] and CCR [49]. We train the PSDiff using AdamW [62] optimizer with the initial learning rate as 2.5×10^{-5} and the weight decay as 10^{-4} . The default training schedule is 90K iterations, with the learning rate divided by 10 at 70K and 84K iterations. The input images are resized to 1333×800 by default. If not specified, s_1 , s_2 and λ_{reid} are set to 2.0, 3.0 and 5.0, respectively. Both N_{train} and N_{test} are set to 300. We employ DDIM as the fast sampling method and inference steps are 8 by default. Following [16], [19], [52], $\lambda_{cls} = 2$, $\lambda_{L1} = 5$, $\lambda_{giou} = 2$. The network is trained with a mini-batch size 32 on 4 NVIDIA V100 and all experiments are implemented on the PyTorch framework.

B. Comparison to the State-of-the-art

In this section, we compare the proposed method with current state-of-the-art (SOTA) methods, including two-stage

TABLE I: Comparison of mAP and top-1 performance with the state-of-the-art methods on CUHK-SYSU and PRW.

Methods		CUHK		PRW		
		mAP	top-1	mAP	top-1	
two-stage	DPM(CVPR'17) [2]	-	-	20.5	48.3	
	RCAA(ECCV'18) [63]	79.3	81.3	-	-	
	RDLR(ICCV'19) [25]	93.0	94.2	42.9	70.2	
	MGTS(TIP'20) [7]	83.0	83.7	32.6	72.1	
	IGPN(CVPR'20) [12]	90.3	91.4	47.2	87.0	
	TCTS(CVPR'20) [26]	93.9	95.1	46.8	87.5	
	OR(TIP'21) [64]	92.3	93.8	52.3	71.5	
	CCR(TIP'23) [65]	93.1	93.7	54.5	89.5	
end-to-end	OIM(CVPR'17) [11]	75.5	78.7	21.3	49.4	
	CTXG(CVPR'19) [66]	84.1	86.5	33.4	73.6	
	HOIM(AAAI'20) [67]	89.7	90.8	39.8	80.4	
	BiNet(CVPR'20) [68]	90.0	90.7	45.3	81.7	
	NAE+(CVPR'20) [9]	92.1	92.9	44.0	81.1	
	DKD(AAAI'21) [59]	93.1	94.2	50.5	87.1	
	PGA(CVPR'21) [69]	90.2	91.8	42.5	83.5	
	AGWF(ICCV'21) [70]	93.3	94.2	53.3	87.7	
	SeqNet(AAAI'21) [10]	93.8	94.6	46.7	83.4	
	Align(CVPR'21) [11]	93.1	93.4	45.9	81.9	
	PSTR(CVPR'22) [13]	93.5	95.0	49.5	87.8	
	COAT(CVPR'22) [14]	94.2	94.7	53.3	87.4	
	OIMN(ECCV'22) [71]	93.1	93.9	46.8	83.9	
	PSDiff (step-1)	90.8	92.1	49.9	80.4	
	PSDiff (step-2)	92.5	93.8	51.1	83.2	
	PSDiff (step-4)	94.7	95.1	52.7	86.3	
	PSDiff (step-8)	95.1	95.3	53.5	87.1	
	Improved backbone					
	PGA-Dilation [69]	92.3	94.7	44.2	85.2	
	Align-DC [11]	94.0	94.5	46.1	82.1	
PSTR-PVTv2 [13]	95.2	96.2	56.5	89.7		
OIMN-Norm [71]	93.1	94.1	47.7	84.8		
PSDiff-Swin (step-8)	95.7	96.3	57.1	88.1		

TABLE II: Complexity and inference speed comparisons.

Methods	Params	Flops	FPS
NAE [9]	33M	575G	14
SeqNet [10]	48M	550G	12
AlignPS [11]	42M	380G	16
RDLR [25]	-	-	15
PSTR [13]	43M	356G	18
COAT [14]	37M	473G	11
PSDiff (step-1)	31M	301G	31
PSDiff (step-2)	31M	309G	27
PSDiff (step-4)	31M	333G	21
PSDiff (step-8)	31M	390G	14

and end-to-end, on the two benchmark datasets. For the two-stage approach, we choose 8 baselines that exhibit excellent performance, including DPM [2], RCAA [63], RDLR [25], MGTS [7], IGPN [12], TCTS [26], OR [64] and CCR [65]. We also compare our methods with 13 end-to-end baselines, such as NAE [9], AlignPS [11], COAT [14], *etc.*

1) *Evaluation On CUHK-SYSU dataset:* Table I shows the performance comparisons on the CUHK-SYSU dataset. The proposed PSDiff achieves 90.8% mAP without refinement (*i.e.*, step-1), which has a performance margin with SOTA methods. However, the performance of PSDiff can be improved significantly with iterative and collaborative refinements. As shown in the gray block of Table I, our PSDiff achieves 95.1% mAP and 95.3% top-1 accuracy with 8 iterative steps, outperforming existing SOTA methods. Moreover, some methods employ improved backbones for better performance, *i.e.*, R50-Dilation

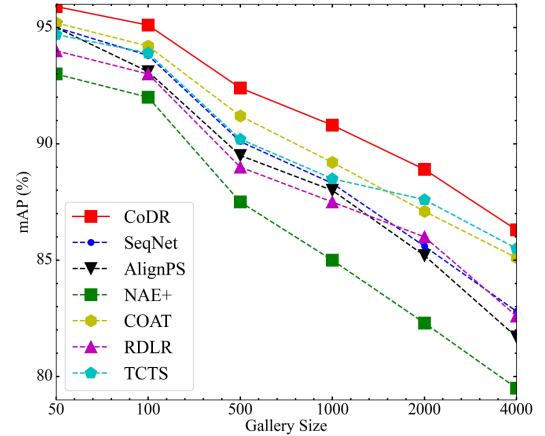


Fig. 4: Comparison to different methods on CUHK-SYSU under varying gallery sizes.

TABLE III: Comparison of transferability with other methods.

Methods	CUHK→PRW		PRW→CUHK	
	mAP	top-1	mAP	top-1
SeqNet [10]	31.4	79.1	55.1	57.3
AlignPS [11]	27.9	77.4	43.6	47.2
COAT [14]	29.0	77.8	56.9	59.4
DAPS [72]	30.3	77.7	52.5	54.8
PSDiff (step-8)	35.5	82.1	58.2	63.7

in [69], deformable convolution (DC) in [11], transformer in [13] and ProtoNorm in [71]. For a fair comparison, we also replace ResNet50 with Swin-B [48] to boost performance. As shown in the bottom of Table I, PSDiff achieves 95.7% mAP and 96.3% top-1 accuracy, outperforming strong methods such as Align-DC [11] and PSTR-PVTv2 [13].

To evaluate the performance scalability of methods, we also compare with other competitive methods under varying gallery sizes of [50, 100, 500, 1000, 2000, 4000] in Fig. 4. A larger gallery size corresponds to a larger search scope, meaning that more distracting people are involved in matching, which is closer to real-world applications. When the gallery size increases, our method still outperforms all existing methods, indicating that our method can handle more challenging real-world situations.

2) *Evaluation On the PRW dataset:* We also show comparisons on the PRW dataset in Table I. PRW is more challenging because of less training data and a larger gallery size, which causes poor performance of mAP in existing methods. Surprisingly, our proposed PSDiff reaches the best performance on mAP, *i.e.*, 53.5% with ResNet-50 and 57.1% with Swin-Base, demonstrating its efficacy under various scenarios. We also note that PSTR [13] obtains the best performance on top-1 accuracy. However, it needs to train three detection decoders and a ReID shared decoder with the multi-level supervision scheme, suffering from the high parameter complexity. In contrast, our PSDiff only trains a single prediction layer and the new paradigm enables us to reuse network parameters.

3) *Efficiency Comparison:* To show the properties of our method on efficiency, we report the complexity of parameters (Params) and computation (Flops) in Table II. We also report the inference speed (FPS) that is computed on the same Tesla

TABLE IV: Ablation experiments of the proposed PSDiff. (a) **Signal-to-Noise Ratios**: s_1, s_2 are the SNR corresponding to detection and ReID tasks. (b) **Collaborative Interaction**: “SA”, “DC” and “CA” refer to the self-attention module, dynamic convolution and cross-attention module in collaborative interaction, respectively. (c) **Cascaded Prediction**.

(a)					(b)					(c)		
$s_1 \backslash s_2$	1.0	2.0	3.0	4.0	SA	DC	CA	mAP	top-1	Methods	mAP	top-1
1.0	93.9	94.0	94.3	93.3				91.3	91.8	parallel(step-1)	90.5	91.7
2.0	94.2	94.6	95.1	94.4	✓			92.5	93.3	parallel(step-8)	93.5	94.1
3.0	94.1	94.2	94.5	94.1	✓	✓		93.8	94.3	cascaded(step-1)	90.8	92.1
4.0	93.8	94.0	94.1	93.8	✓		✓	94.3	94.7	cascaded(step-8)	95.1	95.3
					✓	✓	✓	95.1	95.3			

TABLE V: Comparative results using different inference strategies, *i.e.*, DDIM, DPM-solver and DPM-solver++.

Methods	step-1	step-2	step-4	step-8
DDIM	90.8	92.5	94.7	95.1
DPM-solver	90.8	92.8	94.9	95.1
DPM-solver++	90.8	92.5	94.8	95.0

TABLE VI: Results of different state-of-the-art Re-ID models as the teacher model in the PSDiff. The results on the left represent the performance obtained by utilizing teacher models through traditional distillation methods, while the underlined results on the right show the performance achieved by integrating the teacher model into our diffusion-based architecture.

Methods	mAP	top-1
S-ReID [73] + PSDiff	92.1 / <u>93.5</u>	93.0 / <u>94.1</u>
MGN [74] + PSDiff	92.7 / <u>93.9</u>	92.3 / <u>93.6</u>
AGW [75] + PSDiff	91.9 / <u>93.1</u>	92.5 / <u>93.7</u>
PPLR [76] + PSDiff	93.2 / <u>94.3</u>	93.0 / <u>93.9</u>
HHCL [50] + PSDiff	94.0 / 95.1	93.9 / 95.3

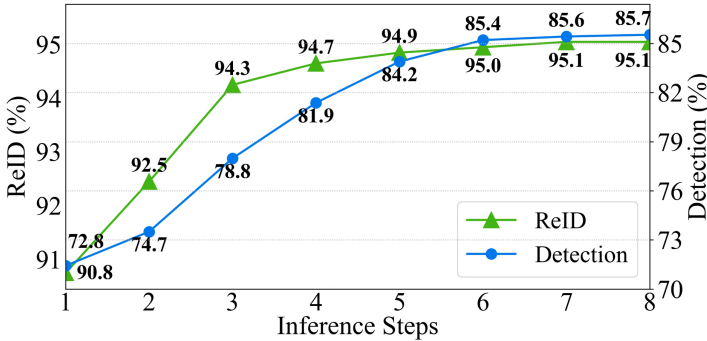


Fig. 5: Performance with increasing steps.

V100 GPU to conduct a fair comparison. As shown in Table II, our PSDiff has the fewest parameters because we only need to train a single denoising layer. Moreover, with the mechanism of iterative and collaborative refinements, our method can achieve elastic computing overhead. Once the model is trained, it can be used by changing inference steps to obtain the best speed-accuracy trade-off under given computing budgets.

4) *Transferability Comparison*: As illustrated in Table III, we assess the model’s performance across datasets without any additional fine-tuning. The results show that previous methods suffer from a severe decline in performance when applied to new datasets. In contrast, our approach sets a new standard by achieving the best results in cross-dataset evaluations. These findings demonstrate that our diffusion-based architecture achieves not only improved performance within the dataset but also exhibits exceptional transferability across different datasets. The remarkable transferability of DiffPS suggests that it serves as an effective method for person search tasks across a wide range of scenarios, *e.g.*, from sparsely populated areas to densely crowded environments, all without necessitating further fine-tuning.

C. Ablation Study

In this section, we conduct extensive experiments on CUHK-SYSU to study PSDiff in detail. First, we analyze the effect of signal-to-noise ratios. Second, we show the effectiveness of our proposed collaborative interaction and cascaded prediction in CDL. Third, we further explore the effect of varying inference steps and fast sampling methods.

1) *Signal-to-Noise Ratios*: As proposed in [19], [36], SNR has a significant effect on performance, especially for different tasks. Therefore, we study the influence of SNR for person search in Table IV (a). Results demonstrate that SNR of $s_1 = 2.0$ for detection and $s_2 = 3.0$ for ReID achieve the best performance. Unlike the task of dense prediction that employs low SNR, *e.g.*, 0.1 for panoptic segmentation [36], higher SNR means the denoising task for person search requires an easier training objective.

2) *Collaborative Interaction*: We investigate the effectiveness of collaborative interaction in CDL. As shown in Table IV (b), the self-attention module can enhance detection features by reasoning about their visual relations, improving 1.2% and 1.5% on mAP and top-1. What’s more, both interactions of the dynamic convolution and the cross-attention module are verified to be essential. Finally, the collaborative interaction significantly boosts the performance by 3.8% and 3.5% on mAP and top-1, respectively.

3) *Cascaded prediction*: To evaluate the effectiveness of the proposed cascaded prediction, we also implement the comparison with “Parallel” strategy. As shown in Table IV (c), our method performs better than the parallel prediction, especially for multi-steps inference. The proposed cascaded prediction outperforms the parallel prediction by 1.6% mAP

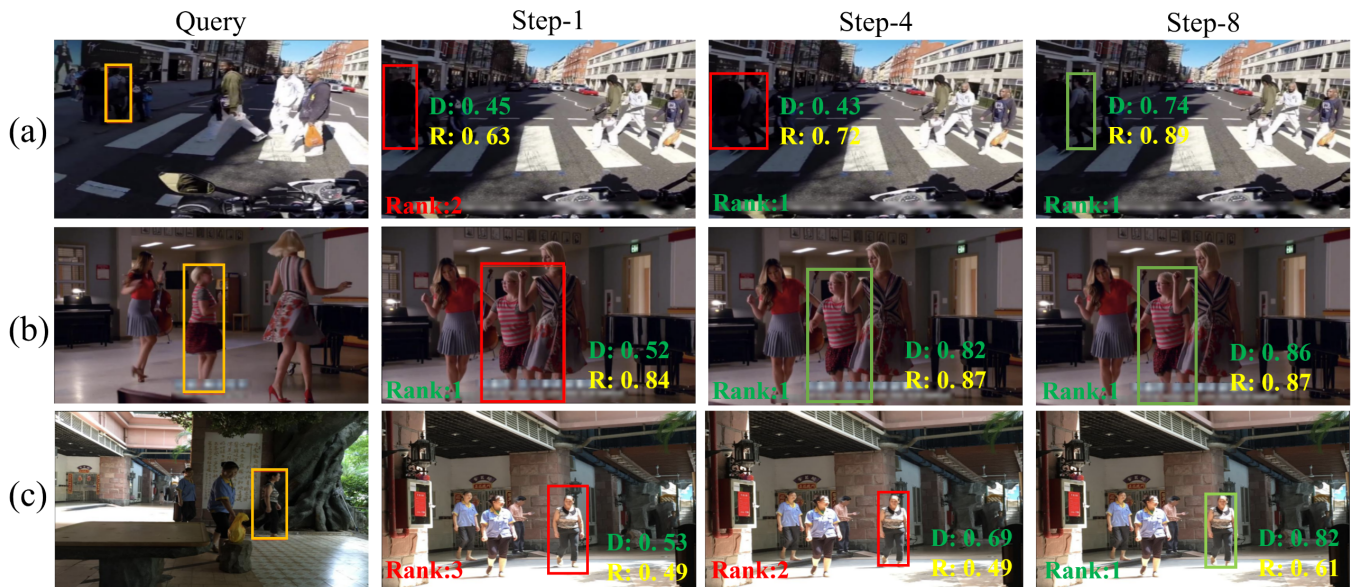


Fig. 6: Qualitative search results on the CUHK-SYSU dataset. The bounding boxes in yellow denote the queries while green and red denote the correct and wrong results. “D” and “R” index confidence scores of detection and ReID matching scores with queries, respectively. “Rank-n” refers to the rank of the presented results among all predictions of the gallery.

and 1.6% top-1 accuracy, which demonstrates the superiority of our cascaded prediction.

4) *Iterative Inference*: We first compare different fast sampling strategies in Table V. Results show more advanced methods, *i.e.*, DPM-solver and DPM-solver++, bring slight benefits, indicating that the diffusion process for person search is insensitive with fast sampling methods. However, DPM-solver and DPM-solver++ are the high-order form of DDIM [57], [58], which causes a decrease in efficiency. Therefore, this paper employs DDIM as the fast sampling strategy. Then, we evaluate PSDiff with different inference steps in Fig. 5. Thanks to our iterative and collaborative refinement, both the performance of detection and ReID are significantly improved with increasing steps, especially for detection performance, *i.e.*, from 72.8% to 85.7% on mAP50. It demonstrates that two sub-tasks should collaboratively work to benefit each other. We also note that the performance remains stable after 6 steps. It is very similar to DDIM for the generative task [45], where images generated with only 20 steps are slightly different from those generated with 1000 steps.

D. Influence of Teacher Models in KD-based vs Diffusion-Based Approaches

Table VI showcases the impact of employing different teacher models on the performance of the person search task. Notably, HHCL stands out with the best performance, owing to its effective use of hard samples and unlabeled samples. More importantly, when applying various methods as the teacher, our diffusion-based architecture consistently outperforms traditional distillation methods, generally by a margin of 1-2%. This highlights the robustness and effectiveness of our proposed framework. Unlike existing approaches that primarily rely on rigid mimicking, the denoising capabilities

inherent in our diffusion framework play a more pivotal role in enhancing the discrimination of the generated embeddings.

E. Qualitative Results

Fig. 6 visualizes the predicted detection and ReID results with increasing inference steps. As shown in cases in Fig. 6, each inference step gradually and collaboratively refines the position and confidence of predicted boxes and the matching score of predicted ReID embeddings. With our collaborative design, not only more accurate detection results contribute to learning more discriminative ReID embeddings, *e.g.*, case (a) and case (c), but also more discriminative ReID clues help refine the position of predicted boxes and improve their confidence scores, *e.g.*, case (b). After multiple refinements, final predictions are more accurate than primary predictions.

VI. CONCLUSION

In this work, we propose a novel diffusion-based person search framework, PSDiff, which formulates the task as a dual denoising process from noisy boxes and noisy ReID embeddings to ground truths. Following the new paradigm, the newly designed CDL enables us to reuse network parameters to refine predictions in an iterative and collaborative way, which also helps obtain the desired speed-accuracy trade-off. PSDiff successfully addresses challenges in previous works, *i.e.*, destructive detection-prior modules and missing collaboration. Experiments on standard benchmarks show the PSDiff achieves SOTA performance with fewer parameters and elastic computing overhead. As a novel work in applying the diffusion model to the person search task, we aim to complement the scarce literature and provide a novel perspective for future research in this field.

ACKNOWLEDGMENT

This work is supported by the National Key Research and Development Program of China (No. 2022YFB3102600), National Nature Science Foundation of China (No. 62192781, No. 62272374, No. 62202367, No. 62250009, No. 62137002), Innovative Research Group of the National Natural Science Foundation of China (61721002), Innovation Research Team of Ministry of Education (IRT_17R86), Project of China Knowledge Center for Engineering Science and Technology, Project of Chinese academy of engineering “The Online and Offline Mixed Educational Service System for ‘The Belt and Road’ Training in MOOC China”, and the K. C. Wong Education Foundation.

REFERENCES

- [1] T. Xiao, S. Li, B. Wang, L. Lin, and X. Wang, “Joint detection and identification feature learning for person search,” in *IEEE Conf. Comput. Vis. Pattern Recog.*, 2017.
- [2] L. Zheng, H. Zhang, S. Sun, M. Chandraker, Y. Yang, and Q. Tian, “Person re-identification in the wild,” in *IEEE Conf. Comput. Vis. Pattern Recog.*, July 2017.
- [3] H. Liu, J. Feng, M. Qi, J. Jiang, and S. Yan, “End-to-end comparative attention networks for person re-identification,” *IEEE Transactions on Image Processing*, vol. 26, no. 7, pp. 3492–3506, 2017.
- [4] L. Zheng, Y. Huang, H. Lu, and Y. Yang, “Pose-invariant embedding for deep person re-identification,” *IEEE Transactions on Image Processing*, vol. 28, no. 9, pp. 4500–4509, 2019.
- [5] Z. Zhong, L. Zheng, Z. Zheng, S. Li, and Y. Yang, “Camstyle: A novel data augmentation method for person re-identification,” *IEEE Transactions on Image Processing*, vol. 28, no. 3, pp. 1176–1190, 2019.
- [6] A. Wu, W.-S. Zheng, and J.-H. Lai, “Robust depth-based person re-identification,” *IEEE Transactions on Image Processing*, vol. 26, no. 6, pp. 2588–2603, 2017.
- [7] D. Chen, S. Zhang, W. Ouyang, J. Yang, and Y. Tai, “Person search by separated modeling and a mask-guided two-stream cnn model,” *IEEE Transactions on Image Processing*, vol. 29, pp. 4669–4682, 2020.
- [8] Y. Yan, Q. Zhang, B. Ni, W. Zhang, M. Xu, and X. Yang, “Learning context graph for person search,” in *IEEE Conf. Comput. Vis. Pattern Recog.*, 2019, pp. 2158–2167.
- [9] D. Chen, S. Zhang, J. Yang, and B. Schiele, “Norm-aware embedding for efficient person search,” in *IEEE Conf. Comput. Vis. Pattern Recog.*, 2020.
- [10] Z. Li and D. Miao, “Sequential end-to-end network for efficient person search,” in *AAAI*, vol. 35, no. 3, 2021, pp. 2011–2019.
- [11] Y. Yan, J. Li, J. Qin, S. Bai, S. Liao, L. Liu, F. Zhu, and L. Shao, “Anchor-free person search,” in *IEEE Conf. Comput. Vis. Pattern Recog.*, 2021, pp. 7690–7699.
- [12] W. Dong, Z. Zhang, C. Song, and T. Tan, “Instance guided proposal network for person search,” in *CVPR*, 2020, pp. 2585–2594.
- [13] J. Cao, Y. Pang, R. M. Anwer, H. Cholakkal, J. Xie, M. Shah, and F. S. Khan, “Pstr: End-to-end one-step person search with transformers,” *Proc. IEEE Conference on Computer Vision and Pattern Recognition*, 2022.
- [14] R. Yu, D. Du, R. LaLonde, D. Davila, C. Funk, A. Hoogs, and B. Clipp, “Cascade transformers for end-to-end person search,” in *IEEE Conference on Computer Vision and Pattern Recognition*, 2022.
- [15] S. Ren, K. He, R. Girshick, and J. Sun, “Faster R-CNN: Towards real-time object detection with region proposal networks,” in *Adv. Neural Inform. Process. Syst.*, 2015.
- [16] N. Carion, F. Massa, G. Synnaeve, N. Usunier, A. Kirillov, and S. Zagoruyko, “End-to-end object detection with transformers,” in *Computer Vision—ECCV 2020: 16th European Conference, Glasgow, UK, August 23–28, 2020, Proceedings, Part I 16*. Springer, 2020, pp. 213–229.
- [17] J. Ho, A. Jain, and P. Abbeel, “Denoising diffusion probabilistic models,” *Advances in Neural Information Processing Systems*, vol. 33, pp. 6840–6851, 2020.
- [18] E. A. Brempont, S. Kornblith, T. Chen, N. Parmar, M. Minderer, and M. Norouzi, “Denoising pretraining for semantic segmentation,” in *Proceedings of the IEEE/CVF Conference on Computer Vision and Pattern Recognition (CVPR) Workshops*, June 2022, pp. 4175–4186.
- [19] S. Chen, P. Sun, Y. Song, and P. Luo, “Diffusiondet: Diffusion model for object detection,” *arXiv preprint arXiv:2211.09788*, 2022.
- [20] F. Gurkan, L. Cerkezi, O. Cirakman, and B. Gunsel, “Tdiot: Target-driven inference for deep video object tracking,” *IEEE Transactions on Image Processing*, vol. 30, pp. 7938–7951, 2021.
- [21] X. Li, M. Chen, and Q. Wang, “Quantifying and detecting collective motion in crowd scenes,” *IEEE Transactions on Image Processing*, vol. 29, pp. 5571–5583, 2020.
- [22] V. Drouard, R. Horaud, A. Deleforge, S. Ba, and G. Evangelidis, “Robust head-pose estimation based on partially-latent mixture of linear regressions,” *IEEE Transactions on Image Processing*, vol. 26, no. 3, pp. 1428–1440, 2017.
- [23] X. Deng, Y. Zhang, J. Shi, Y. Zhu, D. Cheng, D. Zuo, Z. Cui, P. Tan, L. Chang, and H. Wang, “Hand pose understanding with large-scale photo-realistic rendering dataset,” *IEEE Transactions on Image Processing*, vol. 30, pp. 4275–4290, 2021.
- [24] X. Chang, Z. Ma, M. Lin, Y. Yang, and A. G. Hauptmann, “Feature interaction augmented sparse learning for fast kinect motion detection,” *IEEE Transactions on Image Processing*, vol. 26, no. 8, pp. 3911–3920, 2017.
- [25] C. Han, J. Ye, Y. Zhong, X. Tan, C. Zhang, C. Gao, and N. Sang, “Re-id driven localization refinement for person search,” in *Int. Conf. Comput. Vis.*, 2019, pp. 9814–9823.
- [26] C. Wang, B. Ma, H. Chang, S. Shan, and X. Chen, “Tcts: A task-consistent two-stage framework for person search,” in *CVPR*, 2020, pp. 11 952–11 961.
- [27] C. Zhu and Y. Peng, “A boosted multi-task model for pedestrian detection with occlusion handling,” *IEEE Transactions on Image Processing*, vol. 24, no. 12, pp. 5619–5629, 2015.
- [28] X. Zhang, L. Cheng, B. Li, and H.-M. Hu, “Too far to see? not really!—pedestrian detection with scale-aware localization policy,” *IEEE Transactions on Image Processing*, vol. 27, no. 8, pp. 3703–3715, 2018.
- [29] J. Xie, Y. Pang, M. H. Khan, R. M. Anwer, F. S. Khan, and L. Shao, “Mask-guided attention network and occlusion-sensitive hard example mining for occluded pedestrian detection,” *IEEE Transactions on Image Processing*, vol. 30, pp. 3872–3884, 2021.
- [30] Y. Song, J. Sohl-Dickstein, D. P. Kingma, A. Kumar, S. Ermon, and B. Poole, “Score-based generative modeling through stochastic differential equations,” in *International Conference on Learning Representations*, 2021. [Online]. Available: <https://openreview.net/forum?id=PxtIG12RRHS>
- [31] P. Dhariwal and A. Nichol, “Diffusion models beat gans on image synthesis,” *Advances in Neural Information Processing Systems*, vol. 34, pp. 8780–8794, 2021.
- [32] R. Rombach, A. Blattmann, D. Lorenz, P. Esser, and B. Ommer, “High-resolution image synthesis with latent diffusion models,” in *Proceedings of the IEEE/CVF Conference on Computer Vision and Pattern Recognition*, 2022, pp. 10 684–10 695.
- [33] A. Nichol, P. Dhariwal, A. Ramesh, P. Shyam, P. Mishkin, B. McGrew, I. Sutskever, and M. Chen, “Glide: Towards photorealistic image generation and editing with text-guided diffusion models,” *arXiv preprint arXiv:2112.10741*, 2021.
- [34] C. Saharia, J. Ho, W. Chan, T. Salimans, D. J. Fleet, and M. Norouzi, “Image super-resolution via iterative refinement,” *IEEE Transactions on Pattern Analysis and Machine Intelligence*, 2022.
- [35] T. Amit, E. Nachmani, T. Shaharabany, and L. Wolf, “Segdiff: Image segmentation with diffusion probabilistic models,” *arXiv preprint arXiv:2112.00390*, 2021.
- [36] T. Chen, L. Li, S. Saxena, G. Hinton, and D. J. Fleet, “A generalist framework for panoptic segmentation of images and videos,” *arXiv preprint arXiv:2210.06366*, 2022.
- [37] X. Han, H. Zheng, and M. Zhou, “Card: Classification and regression diffusion models,” in *Thirty-Sixth Conference on Neural Information Processing Systems*, 2022.
- [38] W. H. Pinaya, M. S. Graham, R. Gray, P. F. Da Costa, P.-D. Tudosiu, P. Wright, Y. H. Mah, A. D. MacKinnon, J. T. Teo, R. Jager *et al.*, “Fast unsupervised brain anomaly detection and segmentation with diffusion models,” in *Medical Image Computing and Computer Assisted Intervention—MICCAI 2022: 25th International Conference, Singapore, September 18–22, 2022, Proceedings, Part VIII*. Springer, 2022, pp. 705–714.
- [39] J. Wolleb, F. Bieder, R. Sandkühler, and P. C. Cattin, “Diffusion models for medical anomaly detection,” in *Medical Image Computing and Computer Assisted Intervention—MICCAI 2022: 25th International Conference, Singapore, September 18–22, 2022, Proceedings, Part VIII*. Springer, 2022, pp. 35–45.

- [40] J. Wyatt, A. Leach, S. M. Schmon, and C. G. Willcocks, "Anoddp: Anomaly detection with denoising diffusion probabilistic models using simplex noise," in *2022 IEEE/CVF Conference on Computer Vision and Pattern Recognition Workshops (CVPRW)*, 2022, pp. 649–655.
- [41] K. Pandey, A. Mukherjee, P. Rai, and A. Kumar, "Diffusevae: Efficient, controllable and high-fidelity generation from low-dimensional latents," *arXiv preprint arXiv:2201.00308*, 2022.
- [42] J. Ho, C. Saharia, W. Chan, D. J. Fleet, M. Norouzi, and T. Salimans, "Cascaded diffusion models for high fidelity image generation," *J. Mach. Learn. Res.*, vol. 23, no. 47, pp. 1–33, 2022.
- [43] J. Sohl-Dickstein, E. Weiss, N. Maheswaranathan, and S. Ganguli, "Deep unsupervised learning using nonequilibrium thermodynamics," in *International Conference on Machine Learning*. PMLR, 2015, pp. 2256–2265.
- [44] A. Q. Nichol and P. Dhariwal, "Improved denoising diffusion probabilistic models," in *International Conference on Machine Learning*. PMLR, 2021, pp. 8162–8171.
- [45] J. Song, C. Meng, and S. Ermon, "Denoising diffusion implicit models," in *International Conference on Learning Representations*.
- [46] T.-Y. Lin, P. Dollár, R. Girshick, K. He, B. Hariharan, and S. Belongie, "Feature pyramid networks for object detection," in *Proceedings of the IEEE conference on computer vision and pattern recognition*, 2017, pp. 2117–2125.
- [47] K. He, X. Zhang, S. Ren, and J. Sun, "Deep residual learning for image recognition," in *Proceedings of the IEEE conference on computer vision and pattern recognition*, 2016, pp. 770–778.
- [48] Z. Liu, Y. Lin, Y. Cao, H. Hu, Y. Wei, Z. Zhang, S. Lin, and B. Guo, "Swin transformer: Hierarchical vision transformer using shifted windows," in *Proceedings of the IEEE/CVF international conference on computer vision*, 2021, pp. 10 012–10 022.
- [49] C. Jia, M. Luo, C. Yan, X. Chang, and Q. Zheng, "Cgua: Context-guided and unpaired-assisted weakly supervised person search," *arXiv preprint arXiv:2203.14307*, 2022.
- [50] Z. Hu, C. Zhu, and G. He, "Hard-sample guided hybrid contrast learning for unsupervised person re-identification," in *Int. Conf. Comput. Vis.*, 2021.
- [51] Y. Luo, J. Ji, X. Sun, L. Cao, Y. Wu, F. Huang, C.-W. Lin, and R. Ji, "Dual-level collaborative transformer for image captioning," in *Proceedings of the AAAI conference on artificial intelligence*, vol. 35, no. 3, 2021, pp. 2286–2293.
- [52] P. Sun, R. Zhang, Y. Jiang, T. Kong, C. Xu, W. Zhan, M. Tomizuka, L. Li, Z. Yuan, C. Wang *et al.*, "Sparse r-cnn: End-to-end object detection with learnable proposals," in *Proceedings of the IEEE/CVF conference on computer vision and pattern recognition*, 2021, pp. 14 454–14 463.
- [53] Z. Cai and N. Vasconcelos, "Cascade r-cnn: Delving into high quality object detection," in *Proceedings of the IEEE conference on computer vision and pattern recognition*, 2018, pp. 6154–6162.
- [54] R. Stewart, M. Andriluka, and A. Y. Ng, "End-to-end people detection in crowded scenes," in *Proceedings of the IEEE conference on computer vision and pattern recognition*, 2016, pp. 2325–2333.
- [55] T.-Y. Lin, P. Goyal, R. Girshick, K. He, and P. Dollár, "Focal loss for dense object detection," in *Proceedings of the IEEE international conference on computer vision*, 2017, pp. 2980–2988.
- [56] H. Rezatofighi, N. Tsoi, J. Gwak, A. Sadeghian, I. Reid, and S. Savarese, "Generalized intersection over union: A metric and a loss for bounding box regression," in *Proceedings of the IEEE/CVF conference on computer vision and pattern recognition*, 2019, pp. 658–666.
- [57] C. Lu, Y. Zhou, F. Bao, J. Chen, C. Li, and J. Zhu, "Dpm-solver: A fast ode solver for diffusion probabilistic model sampling in around 10 steps," in *Advances in Neural Information Processing Systems*.
- [58] —, "Dpm-solver++: Fast solver for guided sampling of diffusion probabilistic models," *arXiv preprint arXiv:2211.01095*, 2022.
- [59] X. Zhang, X. Wang, J.-W. Bian, C. Shen, and M. You, "Diverse knowledge distillation for end-to-end person search," in *Proc. AAAI Conf. Artif. Intell.*, vol. 35, no. 4, 2021, pp. 3412–3420.
- [60] C. Jia, M. Luo, Z. Dang, X. Chang, and Q. Zheng, "Towards real-time person search with invariant feature learning," in *ICASSP 2023 - 2023 IEEE International Conference on Acoustics, Speech and Signal Processing (ICASSP)*, 2023, pp. 1–5.
- [61] X. Glorot and Y. Bengio, "Understanding the difficulty of training deep feedforward neural networks," in *Proceedings of the thirteenth international conference on artificial intelligence and statistics*. JMLR Workshop and Conference Proceedings, 2010, pp. 249–256.
- [62] I. Loshchilov and F. Hutter, "Decoupled weight decay regularization," *arXiv preprint arXiv:1711.05101*, 2017.
- [63] X. Chang, P.-Y. Huang, Y.-D. Shen, X. Liang, Y. Yang, and A. G. Hauptmann, "Rcaa: Relational context-aware agents for person search," in *Eur. Conf. Comput. Vis.*, 2018, pp. 84–100.
- [64] H. Yao and C. Xu, "Joint person objectness and repulsion for person search," *IEEE Transactions on Image Processing*, vol. 30, pp. 685–696, 2021.
- [65] C. Jia, M. Luo, C. Yan, L. Zhu, X. Chang, and Q. Zheng, "Collaborative contrastive refining for weakly supervised person search," *IEEE Transactions on Image Processing*, pp. 1–1, 2023.
- [66] Y. Yan, Q. Zhang, B. Ni, W. Zhang, M. Xu, and X. Yang, "Learning context graph for person search," in *IEEE Conf. Comput. Vis. Pattern Recog.*, June 2019.
- [67] D. Chen, S. Zhang, W. Ouyang, J. Yang, and B. Schiele, "Hierarchical online instance matching for person search," in *AAAI*, 2020.
- [68] W. Dong, Z. Zhang, C. Song, and T. Tan, "Bi-directional interaction network for person search," in *IEEE Conf. Comput. Vis. Pattern Recog.*, June 2020.
- [69] H. Kim, S. Joung, I.-J. Kim, and K. Sohn, "Prototype-guided saliency feature learning for person search," in *Proceedings of the IEEE/CVF Conference on Computer Vision and Pattern Recognition (CVPR)*, June 2021, pp. 4865–4874.
- [70] B.-J. Han, K. Ko, and J.-Y. Sim, "End-to-end trainable trident person search network using adaptive gradient propagation," in *Int. Conf. Comput. Vis.*, October 2021, pp. 925–933.
- [71] S. Lee, Y. Oh, D. Baek, J. Lee, and B. Ham, "Oimnet++: Prototypical normalization and localization-aware learning for person search," in *European Conference on Computer Vision*. Springer, 2022, pp. 621–637.
- [72] J. Li, Y. Yan, G. Wang, F. Yu, Q. Jia, and S. Ding, "Domain adaptive person search," in *European Conference on Computer Vision*. Springer, 2022, pp. 302–318.
- [73] H. Luo, W. Jiang, Y. Gu, F. Liu, X. Liao, S. Lai, and J. Gu, "A strong baseline and batch normalization neck for deep person re-identification," 2019.
- [74] G. Wang, Y. Yuan, X. Chen, J. Li, and X. Zhou, "Learning discriminative features with multiple granularities for person re-identification," 2018.
- [75] M. Ye, J. Shen, G. Lin, T. Xiang, L. Shao, and S. C. H. Hoi, "Deep learning for person re-identification: A survey and outlook," 2020.
- [76] Y. Cho, W. J. Kim, S. Hong, and S.-E. Yoon, "Part-based pseudo label refinement for unsupervised person re-identification," in *Proceedings of the IEEE/CVF Conference on Computer Vision and Pattern Recognition*, 2022, pp. 7308–7318.



Chengyou Jia received the BS degree in Computer Science and Technology from Xi'an Jiaotong University in 2021. He is currently working toward the Ph. D. degree in Computer Science and Technology at Xi'an Jiaotong University. His research interests include machine learning and optimization, computer vision and multi-modal learning.



Xiaojun Chang is a Professor at Faculty of Engineering and Information Technology, University of Technology Sydney. He is also a visiting Professor at Department of Computer Vision, Mohamed bin Zayed University of Artificial Intelligence (MBZUAI). He was an ARC Discovery Early Career Researcher Award (DECRA) Fellow between 2019-2021. After graduation, he worked as a Postdoc Research Associate in School of Computer Science, Carnegie Mellon University, a Senior Lecturer in Faculty of Information Technology, Monash University, and an Associate Professor in School of Computing Technologies, RMIT University. He mainly worked on exploring multiple signals for automatic content analysis in unconstrained or surveillance videos and has achieved top performance in various international competitions. He received his Ph.D. degree from University of Technology Sydney. His research focus in this period was mainly on developing machine learning algorithms and applying them to multimedia analysis and computer vision.



Minnan Luo received the Ph. D. degree from the Department of Computer Science and Technology, Tsinghua University, China, in 2014. Currently, she is a Professor in the School of Electronic and Information Engineering at Xi'an Jiaotong University. She was a PostDoctoral Research with the School of Computer Science, Carnegie Mellon University, Pittsburgh, PA, USA. Her research interests include machine learning and optimization, cross-media retrieval and fuzzy system.



Jingdong Wang is Chief Scientist for computer vision with Baidu. Before joining Baidu, he was a Senior Principal Researcher at Microsoft Research Asia from September 2007 to August 2021. His areas of interest include vision foundation models, self-supervised pretraining, OCR, human pose estimation, semantic segmentation, image classification, object detection, and large-scale indexing. His representative works include high-resolution network (HRNet) for generic visual recognition, object-contextual representations (OCRNet) for semantic segmentation discriminative regional feature integration (DRFI) for saliency detection, neighborhood graph search (NGS, SPTAG) for vector search. He has been serving/served as an Associate Editor of IEEE TPAMI, IJCV, IEEE TMM, and IEEE TCSVT, and an (senior) area chair of leading conferences in vision, multimedia, and AI, such as CVPR, ICCV, ECCV, ACM MM, IJCAI, and AAAI. He was elected as an ACM Distinguished Member, a Fellow of IAPR, and a Fellow of IEEE, for his contributions to visual content understanding and retrieval.



Zhuohang Dang received a BS degree from the Department of Computer Science and Technology, Xi'an Jiaotong University, in 2021. He is currently working toward the Ph. D. degree in Computer Science and Technology at Xi'an Jiaotong University, supervised by Professor Minnan Luo. His research interests include causal inference and computer vision.



Qinghua Zheng received the B.S. degree in computer software in 1990, the M.S. degree in computer organization and architecture in 1993, and the Ph.D. degree in system engineering in 1997 from Xi'an Jiaotong University, China. He was a postdoctoral researcher at Harvard University in 2002. He is currently a professor in Xi'an Jiaotong University. His research areas include computer network security, intelligent Elearning theory and algorithm, multimedia elearning, and trustworthy software.



Guang Dai received his B.Eng. degree in Mechanical Engineering from Dalian University of Technology and M.Phil. degree in Computer Science from the Zhejiang University and the Hong Kong University of Science and Technology. He is currently a senior research scientist at State Grid Corporation of China. He has published a number of papers at prestigious journals and conferences, e.g., JMLR, AIJ, PR, NeurIPS, ICML, AISTATS, IJCAI, AAAI, ECML, CVPR, ECCV. His main research interests include Bayesian statistics, deep learning, reinforcement learning, and related applications.

ment learning, and related applications.